Investigation of the Carrier Dynamic in GaN-Based Cascade Green Light-Emitting Diodes Using the Very Fast Electrical–Optical Pump–Probe Technique

Jin-Wei Shi, H.-W. Huang, F.-M. Kuo, W.-C. Lai, Ming-Lun Lee, and Jinn-Kong Sheu

***Abstract*—For the first time, the internal carrier dynamic inside GaN-based green light-emitting diodes (LEDs) during operation has been directly observed using the demonstrated electrical–optical pump–probe technique. Short electrical pulses (∼100 ps) were pumped into high-speed cascade green LEDs, and the output optical pulses were probed using high-speed photoreceiver circuits. Using such a method, the recombination time constant of the carriers can be directly measured without any assumption about the recombination process. A high-speed cascade LED structure was adopted in the experiments to eliminate the influence of the RC delay time on the measured responses. Our measurement results indicate that both single- and three-LED cascade structures have the same internal response time due to current continuity. Furthermore, based on responses measured under different temperatures (from 25 °C to 200 °C), the origin of the efficiency droop in GaN-based green LEDs under a high bias current density may be attributed to the strong nonradiative Auger effect rather than device heating or carrier overflow. The demonstrated measurement scheme and high-speed cascade device structure offer a novel and simple way to straightforwardly investigate the internal carrier dynamic inside the active layers of the LED during forward-bias operation.**

***Index Terms*—Carrier dynamic, cascade, efficiency droop, GaN, light-emitting diodes (LEDs).**

I. Introduction

THE STUDY of the internal carrier dynamic and the efficiency droop mechanism in GaN-based blue or violet light-emitting diodes (LEDs) has attracted a lot of attention [1]–[3] due to their applications in next-generation solid-state lighting. The ultrafast optical pump–probe technique is a powerful tool for characterizing the internal carrier dynamic in GaN-based materials and devices derived therefrom [4], [5]. However, this type of technique adopts the femtosecond optical pulse to excite the device under reverse bias, which can eliminate the influence of electroluminescent light from the device on the measurement result. This scheme, thus, does not match the case of LEDs under forward-bias operation with electrical signal injection. A number of theoretical and experimental studies have been carried out in order to better understand the internal carrier dynamic and the origin of the efficiency droop during the operation of GaN-based blue LEDs [1]–[3], [6]. In these works, the internal carrier dynamic is usually analyzed based on the extracted internal and external quantum efficiency (EQE) values of the blue LEDs and the technique of differential carrier lifetime measurement [1]–[3], [7]. However, the internal carrier dynamic, which occurs during the operation of GaN-based LEDs, cannot be so straightforwardly characterized with these approaches. One possible solution to overcome the limitations of the aforementioned techniques is the electrical–optical (E–O) pump–probe technique, where a short electrical pulse (around picoseconds) is injected into the LED during operation, after which we can then measure its output optical pulses by the use of high-speed photoreceiver circuits. These measured impulse responses from the LED definitely represent information about the carrier dynamic inside it. The major challenge of such techniques is that the RC-limited bandwidth of a LED with a large active area (ten thousands of square micrometers) is usually too low to provide a fast enough time resolution. Recently, high-speed GaN-based green LEDs have attracted a lot of attention due to their applications in plastic optical fiber communication and for communication in harsh environments [8], [9]. One can expect a much higher RC-limited bandwidth of such green LEDs compared with the traditional LEDs used for solid-state lighting. In this paper, we investigated the internal carrier dynamic of GaN-based green LEDs using the E–O pump–probe technique. The use of very high speed cascade LEDs with a negligible RC-limited bandwidth [9], [10] and high-speed photoreceiver circuits, which provide a fast enough time resolution, means that such a technique can directly measure the recombination time τ_r of carriers in the multiquantum-well (MQW) layers under different ambient temperatures and bias currents, without making any assumption about the recombination process. Our measurement results indicate that, due to current continuity, both single- and three-LED cascade (serial) structures have exactly the same τ_r inside. In addition, the measured τ_r exhibits very different temperature-dependent behaviors under low and high bias current densities, due to the influence of the piezoelectric (PZ) field inside the MQW layers

Manuscript received June 29, 2010; revised November 6, 2010; accepted November 11, 2010. Date of publication December 13, 2010; date of current version January 21, 2011. This work was supported by the National Science Council of Taiwan under Grants NSC-96-2221-E-008-106-MY3 and 97-2221-E-006-242-MY3. The review of this paper was arranged by Editor L. Lunardi.

J.-W. Shi, H.-W. Huang, and F.-M. Kuo are with the Department of Electrical Engineering, National Central University, Jhongli 320, Taiwan (e-mail: jwshi@ee.ncu.edu.tw).

W.-C. Lai and J.-K. Sheu are with the Institute of Electro-Optical Science and Engineering, National Cheng Kung University, Tainan 701, Taiwan.

M.-L. Lee is with the Department of Electro-Optical Engineering, Southern Taiwan University, Yongkang 710, Taiwan.

Color versions of one or more of the figures in this paper are available online at http://ieeexplore.ieee.org.

Digital Object Identifier 10.1109/TED.2010.2093529

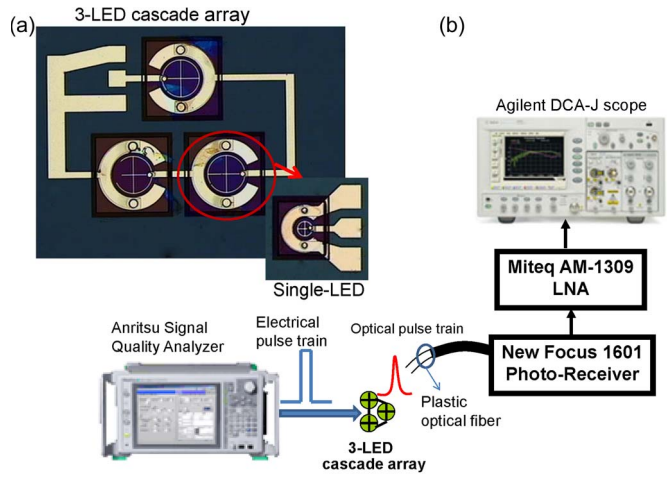

Fig. 1. (a) Top view of the demonstrated LED arrays and a single LED. (b) Setup for impulse response measurement.

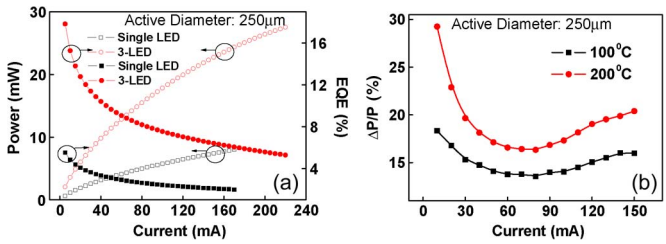

Fig. 2. (a) Measured output power and EQE of single- and three-LED cascade arrays versus bias current. (b) Variation of the measured output power for the same two devices versus bias current under two different ambient temperatures (100 °C and 200 °C).

[11], [12]. Furthermore, under high injection levels, when there is serious efficiency droop, the measured impulse responses show negligible changes even when the ambient temperature increases from room temperature to 200 °C. This result implies that it is likely the strong nonradiative Auger effect that is the origin of the observed efficiency droop of GaN-based green LEDs [13], [14] rather than carrier heating or overflow.

II. Device Structure

The epitaxial layer structures were grown on a (0001) sapphire substrate. The thicknesses of the six-period $In_xGa_{1-x}N$/GaN green MQW region, the bottom n-type GaN (n-GaN) layer, and the topmost p-type GaN layer were about 100, 4000, and 210 nm, respectively. The n-type doping density in some of the GaN barrier layers near the n-type cladding layer was around 7×10^{17} cm^{-3}.

Such n-type barrier doping was used to enhance the modulation speed and output power of the LEDs (for more information, see [12]). A 100-nm-thick n-type (with a doping density of 1×10^{18} cm^{-3}) $In_xGa_{1-x}N$ layer with a mole fraction x ($x = 6\%-8\%$), much less than that of the green MQW layers, was inserted between the bottom n-GaN layer and active MQW layers. This is of benefit to bottom current spreading and improved current–voltage (I–V) characteristics in the fabricated LEDs, which can be attributed to the narrower bandgap, high doping density, and possibly lower resistivity of the inserted InGaN layer than those of the bottom n-GaN layer [15]. Fig. 1(a) shows a top view of the demonstrated three-LED cascade array connected in series. Each LED has an active diameter of around 250 μm. We also fabricated a single LED of the same geometric size as the cascade unit for use as a control device. For details of the cascade LED array fabrication processes, please refer to [9] and [10].

III. Measurement Results and Discussion

The three-LED cascade array exhibits around three times higher output power and EQE than does the single-LED control, at the expense of a threefold increase in the required bias voltage [9], [10]. Fig. 2(a) shows the measured output power and EQE of the single- and three-LED cascade arrays versus bias current. The diameter of the measured LED unit is around 250 μm. As can be seen, the three-LED cascade array exhibits around three times higher output power and external efficiency under the same bias current. High-temperature high-speed operation is an important merit of GaN-based green LEDs. Fig. 2(b) shows the variation of measured output power versus bias current under two different ambient temperatures (100 °C and 200 °C). The values of variation in the output power under different bias currents are normalized to the output power under the corresponding bias currents at room temperature. As can be seen, there is an optimum range (40–80 mA) of bias currents for minimizing the variation in the output power versus temperature. This phenomenon is very different from the behavior of typical semiconductor-based light emitters, which usually exhibit a monotonic increase in the degree of output power degradation with an increase in the bias current, particularly under high-temperature operation. This is due to an increase in the junction temperature (device heating) itself. Our measurement results may be attributed to the influence of defect-related nonradiative recombination or the strong PZ field inside the GaN/InGaN MQW region. Due to the fact that, under a low bias current (< 40 mA), the strong PZ field inside the GaN/InGaN MQW region cannot be completely screened by the space-charge field induced by the external injected current, such an unscreened PZ field consequently lowers the effective barrier height in the MQW region [11], [16]. We thus expect that the effective barrier height increases with the bias current. This should be accompanied by a lower probability of carrier escape and less output power degradation under high-temperature operation. On the other hand, when the bias current exceeds a certain value (> 80 mA), the PZ field is completely screened. The typical temperature-dependent behavior of the light emitter means that the degradation of the output power under high-temperature operation becomes more serious with an increase in the bias current, as is observed in our device. With regard to defect-related nonradiative recombination in the active layers, it usually becomes faster and more serious with an increase in the ambient temperature and leads to the E–O bandwidth enhancement and degradation in EQE of high-speed LEDs under high-temperature operation [17]. In the case of III-nitride-based LEDs, this mechanism usually results in the degradation in EQE under an extremely low bias current density (less than $\sim$10 A/cm^2) [18], [19]. This phenomenon can be minimized

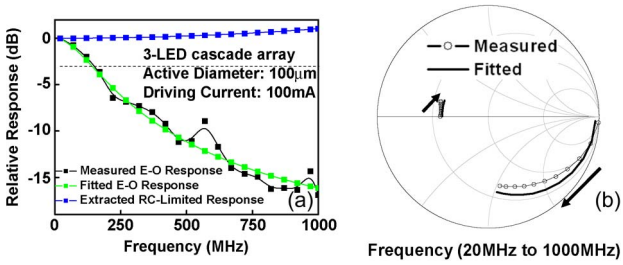

Fig. 3. (a) Measured E–O and extracted RC-limited frequency responses for the single-LED control and the three-LED cascade array under a bias current of 100 mA. (b) Measured and fitted S_{11} parameters (from 20 MHz to 1 GHz) for the three-LED cascade array under forward-bias (a 100-mA bias current) and reverse-bias (-5 V) operations. (Arrowhead) Increase in the sweeping frequency.

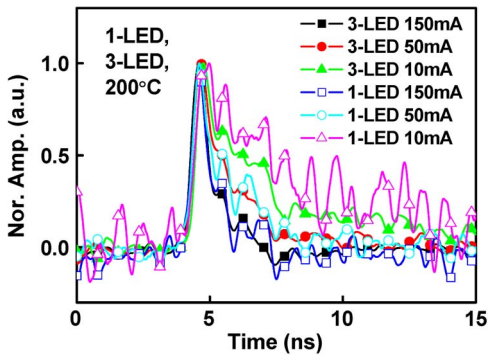

Fig. 4. Measured impulse responses (after normalization) for the single- and three-LED cascade arrays under different bias currents at 200 °C.

by further increasing the bias current to a moderate range ($\sim$20 A/cm^2), and the LED should exhibit the highest value of EQE [18], [19] due to the saturation of the defect states by the external injected carriers. However, for our device, with its small active area, which corresponds to a very high bias current density ($>$ 100 A/cm^2) even under a low bias current (10 mA), defect-related nonradiative recombination may not be the dominant mechanism for the recombination process in the measured impulse responses, as will be discussed later in Figs. 4–6. Furthermore, as shown in Fig. 2(a), the measured EQE of our device monotonically degrades as the bias current increases from low to high (10–200 mA). Such static measurement results are very different from those reported for large-area III-nitride-based LEDs (over 300 $\times$ 300 μm^2) [18], [19], which implies saturation of defect states, even under a low bias current, for our device with a small active area. These static measurement results are consistent with our dynamic measurement results, as will be discussed later. Fig. 1(b) shows a conceptual diagram of our E–O pump–probe measurement setup. During measurement, the device under test (DUT) is mounted on a hot plate for temperature-dependent measurement, where the DUT is injected with different direct-current (dc) bias currents. An electrical pulse train with a full-width at half-maximum of around 100 ps, a 1/64 duty cycle, and a fixed 2-V peak output voltage, which is generated by the programmable pulse pattern generator (Anritsu MP1800 A series), is injected into our device for impulse response measurement. During our experiments, we tried to inject our device with an even shorter electrical pulse. The measured impulse response showed no significant change. This result indicates that the injected electrical pulsewidth is much faster than the internal response time of the LED inside. The optical pulse generated from the DUT was collected by high-speed photoreceiver circuits with a 3-dB bandwidth of approximately 1.5 GHz (New Focus, 1601-AC). This was connected to a 1.5-GHz 3-dB low-noise amplifier (Miteq AM-1309, LNA) and a high-speed sampling scope to record the impulse response. Each cascade unit in the three-LED cascade array used for all dynamic and impulse response measurements (to be discussed later) had an active diameter of 100 μm. Fig. 3(a) shows the measured E–O frequency responses for the single-LED control and the three-LED cascade array under a bias current of 100 mA. As can be seen, although our three-LED cascade structure can have an active area and differential quantum efficiency around three times larger than those of the single control device, both of them have exactly the same 3-dB bandwidth. Under a 100-mA bias current, the measured 3-dB E–O bandwidth is around 250 MHz. Such a result can be attributed to the fact that the cascade structure does not cause the degradation of the RC-limited bandwidth due to the serial connection and the reduction of junction capacitance [9], [10]. The RC-limited bandwidth of the measured cascade LED is extracted by measuring the microwave reflection scattering parameters S_{11} of the three-LED cascade array and then performing the equivalent-circuit modeling technique [20]. Fig. 3(b) shows the measured and fitted S_{11} parameters (from 20 MHz to 1 GHz) for the DUT under forward-bias (a 100-mA bias current) and reverse-bias (-5 V) operations. We can clearly see that the measured and fitted traces match well in the frequency range of interest as obtained using the established equivalent-circuit model. Furthermore, in contrast to the device under reverse-bias operation with a capacitive trace, under forward-bias operation, the device exhibits an inductive trace with a small resistance of around 25 Ω. This result is similar to the reported microwave reflection (S_{11}) parameter of high-speed semiconductor lasers under forward-bias operation [21]. We can now obtain the frequency response under forward-bias operation, as shown by the fitted trace in Fig. 3(a), by using the established inductive-type equivalent-circuit model. The extracted external RC frequency response under forward bias shows a resonant frequency at around 2.8 GHz with a 3-dB bandwidth of around 4 GHz. These numbers are much larger than for the 3-dB bandwidth of the measured E–O frequency response (0.25 GHz). Such a result clearly indicates that the RC-limited frequency response should not have any significant influence on the speed performance of the device or the measured impulse responses (to be discussed later). Fig. 4 shows the measured impulse responses of the single and cascade LEDs under different bias currents. Each trace is normalized to its own maximum values. The traces for the cascade LED are much less noisy and have a better signal-to-noise (S/N) ratio than those of the single LED, particularly under a low bias current (10 mA). This is due to the improvement in EQE of the cascade structure, as discussed in Fig. 2(a). Furthermore, both structures reveal exactly the same internal carrier response time for low to high bias currents (10–150 mA). This is consistent with the results reported for high-speed cascade semiconductor

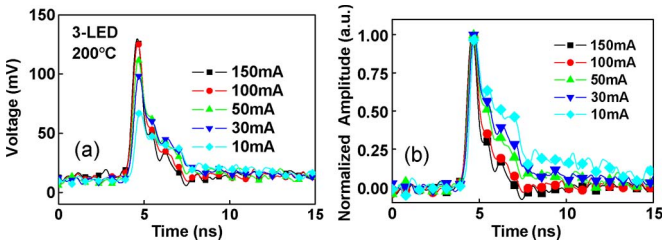

Fig. 5. (a) Measured impulse responses for the three-LED array under different bias currents at 200 °C. (b) Same traces after normalization.

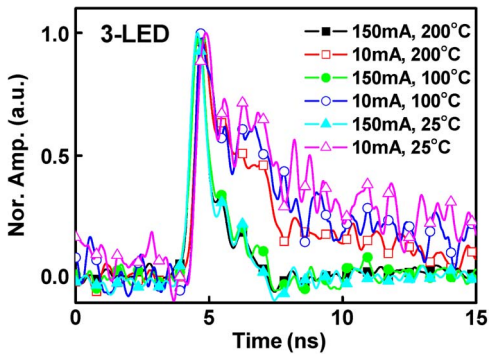

Fig. 6. Measured impulse responses for three-LED cascade arrays (after normalization) under different bias currents (10 and 150 mA) and different ambient temperatures (25 °C, 100 °C, and 200 °C).

lasers [22] and can be attributed to the fact that the bias current is led from one emitter to the next in the cascade arrays with serial connections. Each unit in the cascade array should have the same internal response time and bias current as those of the single device under the same constant current bias. Fig. 5(a) shows the typical measured impulse responses of a three-LED array under different bias currents at 200 °C. Fig. 5(b) shows the same traces after normalization. As can be seen, the measured impulse response greatly shortens with the increase in the dc bias current, accompanied by a significant increase in the peak amplitude under low bias currents (10–50 mA). Although our device is driven under a constant amplitude of the injected voltage pulse (2-V peak to peak), the amplitude of the corresponding current swing should increase with an increase in the dc bias current (output optical power) due to the reduction of the device's differential resistance under forward bias. The increase in the amplitude of the output optical pulse with the increase in the dc bias current (10–50 mA) can thus be measured. However, when the bias current exceeds 50 mA, significant saturation of the peak amplitude can be observed. Such saturation can be attributed not only to the reduction in EQE under a high bias current, as shown in Fig. 2(a), but also to the insignificant reduction in resistance under an extremely high dc bias current ($>$ 100 mA). Based on these measurement results, we can thus conclude that the shortening of the impulse response, particularly under a high bias current ($>$ 100 mA), is due to the enhancement of the nonradiative recombination process (degradation in EQE) with the increase in the bias current. We will discuss this issue in more detail later. Fig. 6 shows the measured impulse responses for a three-LED cascade array (after normalization) under different bias currents (10 and 150 mA) and different ambient temperatures (25 °C, 100 °C,

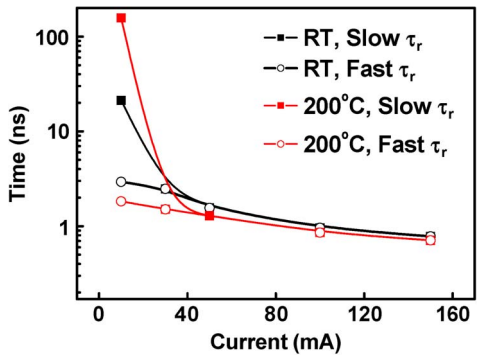

Fig. 7. Extracted τ_r (fall time constants) of measured impulse responses versus bias currents under 25 °C and 200 °C operations.

and 200 °C). We can clearly see that, under high bias currents (150 mA), the measured impulse responses are exactly the same, from low (25 °C) to high ambient temperatures (200 °C). On the other hand, under low bias currents (10 mA), the impulse response significantly shortens with an increase in the ambient temperature. This is consistent with the temperature-dependent measurement results shown in Fig. 2(b).

Under a low bias current ($\sim$10 mA), the strong PZ field in the GaN/InGaN MQW region cannot be completely screened by the external injected current induced space-charge field; therefore, the effective barrier height in the MQW region should be lower [11], [12]. We can thus expect an improvement in device speed with an increase in the ambient temperature due to the increase in the carrier-escaping probability. On the other hand, when the bias current is large enough ($>$ 80 mA) to screen the PZ field inside the MQW region, the effective barrier height should increase, effectively preventing carrier escape from the InGaN wells, even under a high ambient temperature (200 °C).

The invariant impulse responses under a high ambient temperature and a high bias current (density) can thus be measured, as shown in Fig. 6. From these measurement results, we can conclude that it is not carrier heating (escaping) or carrier overflow [2], [3] that induces the shortening of the measured impulse response, particularly under high-temperature operation, leading to the origin of the efficiency droop in our demonstrated GaN-based green LEDs under a high bias current ($>$ 100 mA). Other nonradiative recombination processes, perhaps the Auger effect or defect-related recombination, may be the reasons for the efficiency droop [6], [7], [13], [14]. Although defect-related nonradiative recombination in the active layers usually becomes faster (more serious) with an increase in the ambient temperature [17] and can shorten the measured impulse responses, as what we have measured in Fig. 6, it may not be a major issue for the recombination process in our device, as discussed in Fig. 2. By analyzing the fall time constants of these measured impulse responses, we can further distinguish whether the Auger effect is the dominant mechanism in all the recombination processes. The fall time constants, which can be extracted from these measured impulse responses, definitely represent the recombination time constant τ_r of the internal carrier inside the active MQW layers. This is due to the fact that the RC delay time is not an issue in our cascade LEDs, as shown in Fig. 3. Fig. 7 shows the extracted τ_r versus bias

current (10–150 mA) under 25 °C and 200 °C operations. The corresponding bias current density ranges between 127 and 1900 A/cm^2. As can be seen, under a low bias current (10 mA), we must use two time constants to fit the measured impulse responses. The extracted slow τ_r (> 10 ns) under a low bias current density (127 A/cm^2) can be treated as the time constant for the spontaneous recombination process inside the active MQW layers and is close to the reported value ($\sim$5 ns) for GaN-based blue LEDs operated under the same bias current density ($\sim$100 A/cm^2) at room temperature, as measured by the differential lifetime technique [7]. The observed significant increase in this time constant (20–150 ns) with the increase in the ambient temperature from 25 °C to 200 °C can thus be attributed to the reduction of the radiative (spontaneous) recombination rate under a high ambient temperature [23]. The traces measured under high bias currents (> 30 mA) fit well, just by using a single time constant. Such a fast single time constant can be treated as the Auger recombination time [6], [7], [13], [14], which dominates the total recombination process in InGaN/GaN MQWs operated under such a high bias current density (> 300 A/cm^2) [7]. The τ_r ($\sim$0.8 ns) obtained under a high bias current density (150 mA and 1.9 kA/cm^2) is very close to the reported Auger recombination time constant (less than 1 ns when the bias current density is over 1 kA/cm^2 [7]) in the InGaN/GaN blue MQW regions [7], [14]. On the other hand, in such a high bias current density regime (> 300 A/cm^2), the spontaneous recombination rate tends to be saturated due to the phase-space filling effect [7], leading to it having much less influence on the measured time constant than the Auger effect does [7]. From these static and dynamic measurement results, we can conclude that the dominant mechanism for the efficiency droop in our GaN-based green LEDs operating under high current injection (as well as a high junction temperature) is the Auger recombination process rather than the carrier-heating or the carrier-overflow phenomenon [2], [3]. Contrary to the efficiency droop mechanism reported for GaAs or InP light emitters, which is usually dominated by the carrier-heating effect accompanying the increase in junction temperature [23], the III-nitride-based green LEDs should be less sensitive to this effect. They should have superior high-temperature performance in terms of speed and power [9], due to the much larger bandgap offsets in the InGaN/GaN active MQW regions.

IV. Conclusion

In this paper, we have directly characterized the internal carrier dynamic inside InGaN/GaN-based green LEDs during operation using a very fast E–O pump–probe technique. The influence of the RC delay time on the measured responses is eliminated by adopting a high-speed cascade LED structure in our experiments, as has been verified by the equivalent-circuit modeling technique. Our measurement results indicate that the three-LED cascade structure has exactly the same internal response time but provides a better S/N ratio for the measured traces compared with the single LED. This is due to current continuity through the serial connection and improvement in its power performance, respectively. Furthermore, the measured impulse responses show very different temperature-dependent behaviors under low ($\sim$10 mA) and high bias currents ($\sim$100 mA), which can be attributed to the influence of the strong PZ field inside the InGaN/GaN MQW layers. These dynamic measurement results are consistent with the static temperature-dependent measurement results and indicate that the origin of the efficiency droop in GaN-based green LEDs operating under high bias current densities (> 1 kA/cm^2) can be attributed to the significant nonradiative Auger effect rather than device heating or carrier overflow. The demonstrated measurement scheme and high-speed cascade device structure offer a novel and simple way to straightforwardly investigate the internal carrier dynamic inside the active layers of the LED during forward-bias operation.

References

[1] A. David, M. J. Grundmann, J. F. Kaeding, N. F. Gardner, T. G. Mihopoulos, and M. R. Krames, "Carrier distribution in (0001)InGaN/GaN multiple quantum well light-emitting diodes," *Appl. Phys. Lett.*, vol. 92, no. 5, p. 053 502, Feb. 2008.

[2] M.-H. Kim, M. F. Schubert, Q. Dai, J. K. Kim, E. F. Schubert, J. Piprek, and Y. Park, "Origin of efficiency droop in GaN-based light-emitting diodes," *Appl. Phys. Lett.*, vol. 91, no. 18, p. 183 507, Oct. 2007.

[3] S.-H. Han, D.-Y. Lee, S.-J. Lee, C.-Y. Cho, M.-K. Kwon, S. P. Lee, D. Y. Noh, D.-J. Kim, Y.-C. Kim, and S.-J. Park, "Effect of electron blocking layer in efficiency droop in InGaN/GaN multiple quantum well light-emitting diodes," *Appl. Phys. Lett.*, vol. 94, no. 23, p. 231 123, Jun. 2009.

[4] C.-K. Sun, Y.-L. Huang, S. Keller, U. K. Mishra, and S. P. DenBaars, "Ultrafast electron dynamics in GaN," *Phys. Rev. B, Condens. Matter*, vol. 59, no. 21, pp. 13 535–13 538, Jun. 1999.

[5] K.-G. Gan, C.-K. Sun, S. P. DenBaars, and J. E. Bowers, "Ultrafast valence intersubband hole relaxation in InGaN multiple-quantum-well laser diodes," *Appl. Phys. Lett.*, vol. 84, no. 23, pp. 4675–4677, Jun. 2004.

[6] K. T. Delaney, P. Rinke, and C. G. Van de Walle, "Auger recombination in nitrides form first principles," *Appl. Phys. Lett.*, vol. 94, no. 19, p. 191 109, May 2009.

[7] A. David and M. J. Grundmann, "Droop in InGaN light-emitting diodes: A differential carrier lifetime analysis," *Appl. Phys. Lett.*, vol. 96, no. 10, p. 103 504, Mar. 2010.

[8] J.-W. Shi, J.-K. Sheu, C.-H. Chen, G.-R. Lin, and W.-C. Lai, "High-speed GaN-based green light emitting diodes with partially n-doped active layers and current-confined apertures," *IEEE Electron Device Lett.*, vol. 29, no. 2, pp. 158–160, Feb. 2008.

[9] J.-W. Shi, P.-Y. Chen, C.-C. Chen, J.-K. Sheu, W.-C. Lai, Y.-C. Lee, P.-S. Lee, S.-P. Yang, and M.-L. Wu, "Linear cascade GaN based green light emitting diodes with invariant high-speed/power performance under high-temperature operation," *IEEE Photon. Technol. Lett.*, vol. 20, no. 23, pp. 1896–1898, Dec. 2008.

[10] J.-W. Shi, J.-K. Sheu, C.-K. Wang, C.-C. Chen, C.-H. Hsieh, J.-I. Chyi, and W.-C. Lai, "Linear cascade arrays of GaN based green light emitting diodes for high-speed and high-power performance," *IEEE Photon. Technol. Lett.*, vol. 19, no. 18, pp. 1368–1370, Sep. 2007.

[11] H. Haratizadeh, B. Monemar, P. P. Paskov, J. P. Bergman, B. E. Sernelius, P. O. Holtz, M. Iwaya, S. Kamiyama, H. Amano, and I. Akasaki, "Photoluminescence study of Si-doped GaN/$Al_{0.07}Ga_{0.93}N$ multiple quantum wells with different dopant positions," *Appl. Phys. Lett.*, vol. 84, no. 25, pp. 5071–5073, Jun. 2004.

[12] J.-W. Shi, H.-Y. Huang, J.-K. Sheu, C.-H. Chen, Y.-S. Wu, and W.-C. Lai, "The improvement in modulation speed of GaN-based light-emitting diode (LED) by use of n-type barrier doping for plastic optical fiber (POF) communication," *IEEE Photon. Technol. Lett.*, vol. 18, no. 15, pp. 1636–1638, Aug. 2006.

[13] N. F. Gardner, G. O. Muller, Y. C. Shen, G. Chen, S. Wantanabe, W. Gotz, and M. R. Krames, "Blue-emitting InGaN–GaN double-heterostructure light-emitting diodes reaching maximum quantum efficiency above 200 A/cm^2," *Appl. Phys. Lett.*, vol. 91, no. 24, p. 243 506, Dec. 2007.

[14] Y. C. Shen, G. O. Mueller, S. Watanabe, N. F. Gardner, A. Munkholm, and M. R. Krames, "Auger recombination in InGaN measured by photoluminescence," *Appl. Phys. Lett.*, vol. 91, no. 14, p. 141 101, Oct. 2007.

[15] C.-H. Jang, J.-K. Sheu, C. M. Tsai, S.-J. Chang, W.-C. Lai, M.-L. Lee, T. K. Ko, C. F. Shen, and S. C. Shei, "Improved performance of GaN-based blue LEDs with the InGaN insertion layer between the MQW active layer and the n-GaN cladding layer," *IEEE J. Quantum Electron.*, vol. 46, no. 4, pp. 513–517, Apr. 2010.
[16] J. Piprek, R. Farrell, S. P. DenBaars, and S. Nakamura, "Effects of built-in polarization on InGaN–GaN vertical-cavity surface-emitting lasers," *IEEE Photon. Technol. Lett.*, vol. 18, no. 1, pp. 7–9, Jan. 2006.
[17] M. Pessa, M. Guina, M. Dumitrescu, I. Hirvonen, M. Saarinen, L. Toikkanen, and N. Xiang, "Resonant cavity light emitting diode for a polymer optical fiber system," *Semicond. Sci. Technol.*, vol. 17, no. 6, pp. R1–R9, Jun. 2002.
[18] J. K. Sheu, C. M. Tsai, M. L. Lee, S. C. Shei, and W. C. Lai, "InGaN light-emitting diodes with naturally formed truncated micropyramids on top surface," *Appl. Phys. Lett.*, vol. 88, no. 11, p. 113 505, Mar. 2006.
[19] J.-W. Shi, S.-H. Guol, C.-S. Lin, J.-K. Sheu, K. H. Chang, W.-C. Lai, C.-H. Kuo, C.-J. Tun, and J.-I. Chyi, "The structure of GaN-based transverse junction blue light-emitting diode array for uniform distribution of injected current/carriers," *IEEE J. Sel. Topics Quantum Electron.*, vol. 15, no. 4, pp. 1292–1297, Jul./Aug. 2009.
[20] Y.-S. Wu, J.-W. Shi, and P.-H. Chiu, "Analytical modeling of a high-performance near-ballistic uni-traveling-carrier photodiode at a 1.55 μm wavelength," *IEEE Photon. Technol. Lett.*, vol. 18, no. 8, pp. 938–940, Apr. 2006.
[21] D. A. Tauber, R. Spickermann, R. Nagarajan, T. Reynolds, A. L. Holmes, Jr., and J. E. Bowers, "Inherent bandwidth limits in semiconductor lasers due to distributed microwave effects," *Appl. Phys. Lett.*, vol. 64, no. 13, pp. 1610–1612, Mar. 1994.
[22] P. Modh, S. Galt, J. Gustavsson, S. Jacobsson, and A. Larsson, "Linear cascade VCSEL arrays with high differential efficiency and low differential resistance," *IEEE Photon. Technol. Lett.*, vol. 18, no. 1, pp. 100–102, Jan. 2006.
[23] L. A. Coldren and S. W. Corzine, *Diode Lasers and Photonic Integrated Circuits*. New York: Wiley, 1995, ch. 4.

Jin-Wei Shi was born in Kaohsiung, Taiwan, on January 22, 1976. He received the B.S. degree in electrical engineering and the Ph.D. degree from National Taiwan University, Taipei, Taiwan, in 1998 and 2002, respectively.

He was a Visiting Scholar with the University of California, Santa Barbara, during 2000 and 2001. In 2002–2003, he was a Postdoctoral Researcher with the Electronic Research and Service Organization, Industrial Technology Research Institute. In 2003, he joined the Department of Electrical Engineering, National Central University, Jhongli, Taiwan, where he is currently an Associate Professor. He has authored or coauthored more than 70 journal papers and 100 conference papers. He is the holder of 13 patents. His current research interests include ultrahigh-speed/power optoelectronic devices such as photodetectors, electroabsorption modulators, submillimeter-wave photonic transmitters, and semiconductor lasers.

Dr. Shi was an invited speaker at the 2002 IEEE Lasers and Electro-Optics Society Annual Meeting, the 2005 Society of Photo-Optical Instrumentation Engineers Optics East Symposium, 2007 Asia-Pacific Microwave Photonics Conference, and 2008 Asia Optical Fiber Communication & Optoelectric Expositon & Conference. He has served as a member of the Technical Program Committee for the 2009–2011 Optical Fiber Communication Conference and Exposition. He was the recipient of the 2007 Excellence Young Researcher Award from the Association of Chinese IEEE.

H.-W. Huang was born in Taipei, Taiwan, on February 26, 1985. He received the B.S. degree in electrical engineering from National Chin-Yi University of Technology, Taiping, Taiwan. He is currently working toward the M.S. degree in electrical engineering with National Central University, Jhongli, Taiwan.

His research interests include high-power and high-speed light-emitting diodes.

F.-M. Kuo was born in Kaohsiung, Taiwan, on February 12, 1986. He received the B.S. degree in electrical engineering from National Central University, Jhongli, Taiwan, where he is currently working toward the M.S. degree in electrical engineering.

His research is mainly focused on millimeter-wave high-power photodiodes and their applications. He is also involved in radio-frequency/microwave semiconductor optoelectronic devices for communication, such as vertical-cavity surface-emitting lasers, avalanche photodiodes, and high-speed light-emitting diodes.

W.-C. Lai was born in Taiwan in 1970. He received the M.S. and Ph.D. degrees in electrical engineering from National Cheng Kung University (NCKU), Tainan, Taiwan, in 1995 and 2001, respectively.

In 2001, he was a Postdoctoral Associate with the Department of Electrical Engineering, NCKU. He is currently with the Institute of Electro-Optical Science and Engineering, NCKU, as an Associate Professor. His research interest includes the growth and characterization of III–V nitride semiconductors and devices.

Ming-Lun Lee was born in Taiwan in 1978. She received the M.S. degree in physics from National Central University, Jhongli, Taiwan, in 2002 and the Ph.D. degree from National Cheng Kung University, Tainan, Taiwan, in 2005.

In 2005, she joined the Department of Electro-Optical Engineering, Southern Taiwan University, Yongkang, Taiwan, as an Assistant Professor. She is currently an Associate Professor with the same university. Her research interests include the characterization of III–V compound semiconductors and optoelectronics device fabrication and characterization.

Jinn-Kong Sheu was born in Taiwan in 1970. He received the M.S. and Ph.D. degrees in electrical engineering from National Cheng Kung University (NCKU), Tainan, Taiwan, in 1995 and 1999, respectively.

From 1997 to 2000, he was a Senior Engineer with Epistar Corporation Ltd., specializing in the manufacturing of high-brightness light-emitting diode chips and the growth of epitaxial wafers by metal–organic vapor phase epitaxy. From 2000 to 2003, he was with the Optical Science Center, National Central University, Jhongli, Taiwan, as a Postdoctoral Researcher. From 2003 to 2004, he was an Assistant Professor with the Institute of Optical Science, National Central University. He is currently with the Institute of Electro-Optical Science and Engineering, NCKU, as a Professor. His research interests include the epitaxial growth and characterization of III–V compound semiconductors, optoelectronics device fabrication and characterization, and wide-bandgap compound semiconductor materials and devices.